Research Square

Preprints are preliminary reports that have not undergone peer review.
They should not be considered conclusive, used to inform clinical practice,
or referenced by the media as validated information.

# Predicting Diagnostic Gene Biomarkers Associated with Ferroptosis in Psoriasis

**Juan Yang**
The Fourth Affiliated Hospital of Guangzhou Medical University
**Qing Liu**
The fifth Affiliated Hospital of Guangzhou Medical University
**Xiuyi Lu**
The Fourth Affiliated Hospital of Guangzhou Medical University
**Liuyan Wen**
The Fourth Affiliated Hospital of Guangzhou Medical University
**Shaoping Yuan**
The Fourth Affiliated Hospital of Guangzhou Medical University
**Weiqi Wu** ( 2021689171@gzhmu.edu.cn )
https://orcid.org/0000-0002-6906-1202

**Research**

**Keywords:** Psoriasis, GSVA, WGCNA, Ferroptosis, Diagnostic Gene Biomarker

**Posted Date:** May 24th, 2022

**DOI:** https://doi.org/10.21203/rs.3.rs-1657526/v1

**License:** This work is licensed under a Creative Commons Attribution 4.0 International License.
Read Full License

Manuscript Click here to access/download;Manuscript;Manuscript.tex

Click here to view linked References



RESEARCH

# Predicting Diagnostic Gene Biomarkers Associated with Ferroptosis in Psoriasis

Juan Yang[1,2†], Qing Liu[3†], Xiuyi Lu[1,2], Liuyan Wen[1,2], Shaoping Yuan[1,2] and Weiqi Wu[1,2*]

*Correspondence: 2021689171@gzhmu.edu.cn
[1]Department of dermatology, The Fourth Affiliated Hospital of Guangzhou Medical Universitye, 511300 Guangzhou, China
[2]Department of dermatology, Zengcheng District Pepole's Hospital of Guangzhou, 511300 Guangzhou, China
Full list of author information is available at the end of the article
†Equal contributor

## Abstract

**Background:** Psoriasis is a prevalent, chronic, and recurrent inflammatory disorder, and new research reveals that ferroptosis plays a role in the pathogenic process.

**Methods:** Two microarray datasets (GSE6710 and GSE83582) about psoriasis were collected from the GEO database, and the ferroptosis-related genes were extracted from FerrDb. Enrichment scores associated with ferroptosis were obtained using gene set enrichment analysis (GSEA) and gene set variation analysis (GSVA) in two microarray datasets, and weighted gene co-expression network analysis (WGCNA) was used to identify ferroptosis-associated module genes in psoriasis, and took the intersection of the key modules. Next, the protein-protein interaction (PPI) and Gene Ontology (GO) pathway enrichment analyses, as well as the Kyoto Encyclopedia of Genes and Genomes (KEGG) pathway enrichment studies, were performed. The hub genes were identified using Cytoscape with CytoHubba, and a receiver operator characteristic (ROC) curve was utilized to discriminate psoriasis from controls.

**Results:** Ferroptosis-related hub genes in psoriasis (CXCL8, STAT3 and STAT1) were ultimately discovered, and they were able to discriminate psoriasis from controls. The AUC (area under the ROC curve) was above 0.75. To confirm that CXCL8, STAT1, and STAT3 could effectively differentiate psoriasis from controls, the diagnostic value was further validated in the GSE30999, GSE13355, and GSE78097 datasets. Three hub genes had AUC values that were also above 0.75 in three external datasets.

**Conclusions:** We discovered three hub genes (CXCL8, STAT1, and STAT3) that are linked to ferroptosis in psoriasis and can distinguish psoriasis from controls. As a result, CXCL8, STAT1, and STAT3 might be used as ferroptosis-associated biomarkers for disease diagnosis and treatment monitoring.

**Keywords:** Psoriasis; GSVA; WGCNA; Ferroptosis; Diagnostic Gene Biomarker

## Introduction

Psoriasis is an autoimmune skin disorder that affects 2-3% of the world's population[1]. It is a papulosquamous skin disorder with a well-known morphology of red plaques on the skin that are covered in white or silver scales[1]. The pathogenesis of psoriasis is not fully understood, and it's also debatable whether psoriasis is caused by primary keratinocyte abnormalities, primary immune system dysregulation, or a combination of the two[2]. Psoriatic skin is characterized by abnormal

activation and metabolism of epidermal keratinocytes, which leads to greatly increased keratinocyte proliferation and abnormal terminal differentiation[3]. Keratinocytes are impaired and die as a result of the destruction of the epidermal barrier, which is linked to aberrant cell differentiation and a reduced cellular cycle period[4]. However, the exact process of programmed cell death in psoriasis remains unknown[4].

Ferroptosis is a morphologically and mechanistically different kind of cell death that is produced by excessive lipid peroxidation and is iron-dependent[4, 5]. Ferroptosis has been linked to a variety of disorders, including nervous system and heart problems, because of its function in inflammation and tissue damage[6–8]. According to new findings, ferroptosis may have a role in the psoriasis pathogenic process[4], but few research has been done on the involvement of ferroptosis in psoriasis. Ferroptosis inhibitors have been demonstrated to have anti-inflammatory effects in animal models of acute kidney injury, neurodegenerative diseases and intracerebral hemorrhage[7, 9, 10]. As a result, more investigation into the involvement of ferroptosis in psoriasis pathogenesis is needed. Transcriptomics research has shown promise in recent years in terms of assisting researchers in deepening their grasp of disease causes and efficiently exploring biomarkers[11, 12]. WGCNA (weighted gene co-expression network analysis) is a systematic biological approach for identifying highly synergistically changed gene sets that may be selected out based on the link between gene sets and phenotypes and the intrinsic qualities of gene sets[13].

We used a combination of differentially expressed gene (DEG) analysis, Gene Set Enrichment Analysis (GSEA), Gene Set Variation Analysis (GSVA), and WGCNA to screen out the hub gene in two datasets (GSE6710 and GSE83582), as well as validation in three different datasets (GSE30999, GSE13355, and GSE78097). Finally, three genes (CXCL8, STAT3, and STAT1) were discovered, which could be used as potential diagnostic indicators for psoriasis related to ferroptosis.

## Materials and methods

### Data collection and preprocessing

The Gene Expression Omnibus (GEO, http://www.ncbi.nlm.nih.gov/geo) was searched for human psoriasis microarray datasets. The following were the selection criteria: 1. Skin tissue samples from plaque-type psoriasis patients, including lesional skin and uninvolved skin; 2. Skin tissue samples from plaque-type psoriasis patients and normal healthy skin were included; 3. Datasets should contain at least 20. The GSE6710 and GSE83582 datasets were obtained using these criteria, and annotated using the Affymetrix Human Genome U133A Array platform and the 2.1 ST Array platform. GSE6710 was comprised of uninvolved and involved skin from 13 people with plaque-type psoriasis ranging from mild to severe. GSE83582 contained 20 normal healthy skin biopsies, 12 chronic plaque psoriasis, 40 inverse psoriasis, and 30 erythrodermic psoriasis. We used 12 normal healthy skin biopsies (GSM2209922-GSM2209933) and 12 chronic plaque psoriasis (GSM2209934-GSM2209945). RMA background correction and the “affy" R language package were used for log2 transformation, quantile normalization, and median polish algorithm summarization in the microarray analysis[14]. We matched the probes to gene symbols using probe annotation information. Those probes that matched with more than one gene were removed, and when more than

one probe matched with a gene, its final expression was determined by the greatest expression value. Null genes containing "//" and blanks had been removed. Afterwards, the gene expression profiles were quantile normalized. Besides, a total of 259 FRGs were extracted from the FerrDb website[15](http://www.zhounan.org/ferrdb). Supplementary Figure 1 depicts a flowchart of this research.

### Differentially expressed genes (DEGs)

For the purpose of DEGs between psoriasis samples and normal healthy skin samples, as well as DEGs between uninvolved and lesional skin of plaque psoriasis patients, the R package "Limma" (linear models for microarray data) in R software (version 4.1.3) was used[16]. The DEGs were screened using the following cut-off criteria: adjusted P-value (adj.P.Val) $<0.05$ and $|\ log_2$ Fold Change$|(|\ log_2$ FC $|) >1$, and these DEGs were used to draw maps of the volcanoes using scripts in the R software Ggplot2 package.

### Gene set enrichment analysis (GSEA) of pathways related to ferroptosis

GSEA was conducted between uninvolved and lesional skin of plaque psoriasis patients in GSE6710, as well as between psoriasis samples and normal healthy skin samples in GSE83582. We used all the genes in the two datasets, and 259 FRGs from the FerrDb website were selected as the reference gene set. The R packages "clusterProfiler", "enrichplot", and "GSEABase" in R software 4.1.3 were utilized to conduct GSEA[17, 18]. GSEA were screened using the following cut-off criteria: the FDR (False Discovery Rate) was 0.25, and the adjusted P-value was 0.05.

### Gene set variation analysis (GSVA) to obtain enrichment scores (ES) of ferroptosis -associated pathways

GSVA was conducted between uninvolved and lesional skin of plaque psoriasis patients in GSE6710, as well as between psoriasis samples and normal healthy skin samples in GSE83582. We used all the genes in the two datasets, and chose the 259 FRGs from the FerrDb website as the reference gene set. We used the "GSVA" package in R software 4.1.3 to calculate the ES of each gene set that was correlated with ferroptosis pathways[19].

### Weighted gene co-expression network (WGCN) construction and identification of modules

In order to identify key modules that were correlated with ferroptosis and pathology of plaque psoriasis, the weighted correlation network based on the mRNA expression profiling from GSE6710 and GSE83582 was constructed via the "WGCNA" package in R software 4.1.3[13]. We adopted all the genes in each gene set, enrichment scores of ferroptosis associated pathways and group information to construct the co-expression network. We chose the suitable soft threshold power based on standard scale-free networks and estimated adjacencies by a power function (scale free $R^2$ $=0.9$). Then we obtained the dissimilarity TOM (1-TOM) by transforming the adjacencies into topological overlap matrixes (TOM). By combining the parameters of minModuleSize 50 and

mergeCutHeight 0.25, we used average linkage to conduct hierarchical clustering. Using Pearson's correlation analysis, the clinically important modules were subsequently identified by calculating the association between external clinical information and the module eigengenes (MEs). The association between clinical characteristics and genes, as well as the relationship between MEs and genes, were also investigated. Eventually, the absolute values of module eigengene (ME) in plaque psoriasis and ferroptosis, both top ranked among the modules, were selected as key modules.

### Taking the intersection of key modules

We took the intersection of key genes that were selected from GSE6710 and GSE83582 by WGCNA. Then we obtained co-expression key genes in the two module memberships.

### Protein-protein interaction network building

We used the "STRINGdb" package in R software 4.1.3 to obtain protein-protein interaction information with a score threshold of 400[20]. Then, Cytoscape (version 3.7.2) was used to visualize the results[21]. With 11 scoring methods, the Cytoscape plug-in CytoHubba provides a straightforward interface for analyzing the node essentiality in the specified network[22]. We used the five methods to screen the top 10 genes, then took the intersection of those top 10 genes as hub genes.

### Functional and pathway enrichment analysis of hub genes

The Kyoto Encyclopedia of Genes and Genomes (KEGG) Pathway Enrichment Analysis and Gene Ontology (GO) enrichment analysis of hub genes were performed by applying the "clusterProfiler" package in R software 4.1.3, and we used the following Settings: pvalueCutoff = 0.05, pAdjustMethod = "BH" and ont="ALL"[17].

### Receiver operator characteristic (ROC) curve, expression and validation of the hub genes

To calculate ROC, we utilized the "pROC" package in R software 4.1.3. We created ROC curves and assessed the area under the ROC curve (AUC) to verify the potential diagnostic usefulness of hub genes [23]. Meanwhile, the difference in hub gene expression between lesional skin tissue and control was measured by using the T-test, with $p < 0.05$ being regarded as a significant difference. Furthermore, three distinct external datasets were used to validate the hub genes' expression levels and diagnostic value (GSE78097, GSE30999, and GSE13355).

## Results

### Identification of DEGs

The "Limma" package in R software 4.1.3 was used to analyze the gene expression data. After deleting blank values, and removing repeated and containing "//" genes, GSE6710 yielded a total of 12,539 genes and 26 samples, whereas GSE83582 yielded a total of 19,767 genes and 24 samples. Using the adj.P.Val $<0.05$ and $|\log2\ FC| > 1$ cut-off criteria, 836 genes in GSE6710 were identified as DEGs, while 238 genes in GSE83582 were classified as DEGs. In GSE6710, there were 410 up-regulated DEGs labeled as red plots and 426 down-regulated DEGs labeled as blue plots, while in

GSE83582, there were 179 up-regulated DEGs labeled as red plots and 59 down-regulated DEGs labeled as blue plots. On the volcano map, the DEGs with the most aberrant expression were highlighted (Figure 1A-1B).

### GSEA of pathways related to ferroptosis

GSEA was used to investigate the possible processes of all genes in GSE6710 and GSE83582 in relation to the effects of ferroptosis-related pathways. FDR <0.25 and adj.P.Val <0.05 were used as cut-off values. GSE6710 and GSE83582 have normalized enrichment scores (NES) of 0.33 and 0.39, respectively, with false discovery rates (FDRs) of 0.015 and 0. The findings revealed that the gene sets were considerably enriched in ferroptosis-related pathways (Figure 1C-1D).

### GSVA to obtain the ES of ferroptosis-associated pathways

The ES of each gene set that was connected to ferroptosis pathways was obtained using GSVA, and a summary of the GSVA of each data set is shown in Supplementary table 1.

### WGCNA and key modules identification

To identify the key genes associated with ferroptosis and the development of plaque psoriasis, the GSE6710 and GSE83582 datasets were used to perform co-expression network analysis via WGCNA. A total of 12,539 genes and 26 samples from GSE6710 and a total of 19,767 genes and 24 samples from GSE83582 were input into R software 4.1.3 for WGCNA, and it was used to discover the strongly correlated genes and co-expression networks of ferroptosis and the development of plaque psoriasis. In addition, clinical features (group information, ES of ferroptosis associated pathways) were obtained for WGCNA. Outlier samples were eliminated based on sample clustering, and all samples were eventually enrolled. As a soft threshold for a scale-free network, we chose a power of $\beta$ =3 (scale-free $R^2$ = 0.9) in GSE6710 (Figure 2A) and a power of $\beta$ =5 (scale-free $R^2$ = 0.9) in GSE83582 (Figure 3A). By combining the parameters of minModuleSize 50 and mergeCutHeight 0.25, the hierarchical clustering dendrogram created 10 gene modules in GSE6710, ranging in size from 6,617 (turquoise module) to 166 (purple module) (Figure 2B), while the hierarchical clustering dendrogram identified 58 gene modules in GSE83582, ranging in size from 4,535 (turquoise module) to 58 (skyblue2 and yellow4 module) (Figure 3B).

In order to examine the relationship between clinical characteristics and module eigengene (ME) values, the correlation between clinical features and ME values was used. The heatmap of module-trait correlations showed that the turquoise module in GSE6710 was the most closely correlated with psoriasis (Pearson coefficient = -0.97, P = 5e-17) and ferroptosis (Pearson co-efficient = -0.8, P = 1e-06) (Figure 2C), and that the purple module in GSE83582 was the most closely corrected with psoriasis (Pearson co-efficient = 0.91, P = 5e-10) and ferroptosis (Pearson co-efficient = 0.72, P = 8e-05) (Figure 3E). In addition, the genes in the two selected modules were evaluated for their value and module membership, and we plotted the scatterplots (Figure 2D-2E, Figure 3C-3D). We chose 1000 genes at random to create the network heatmaps that were used to examine

module interaction relationships (Figure 2F, Figure 4A). Furthermore, according to the module eigengene dendrogram, the 10 modules in GSE6710 were mostly separated into two groups, whereas the 58 modules in GSE83582 were mostly separated into two groups, and the eigengene network heatmap revealed comparable outcomes (supplementary Figure 2, Figure 4B). Therefore, we chose the turquoise module in GSE6710 and the purple module in GSE83582 for further investigation to evaluate the module's relevance to clinical aspects of considerable biological importance.

### Taking the intersection of the turquoise module and the purple module

GSE6710 contained 6,617 genes in the turquoise module and GSE83582 contained 468 genes in the purple module. To identify the intersection of the turquoise module and the purple module, the venn diagram analysis was performed using R software 4.1.3. The intersection of the two modules contains 239 genes, as seen in the venn diagram (Figure 5A).

### Protein-protein interaction network building

With a score threshold of 400, we used the "STRINGdb" package in R software 4.1.3 to obtain protein-protein interaction information, and all 239 genes were submitted to construct the PPI network. In the PPI network, there were 238 nodes and 720 edges (Figure 5B). After that, the data was visualized using the Cytoscape (version 3.7.2) plug-in CytoHubba. Radiality, Betweenness, Closeness, Degree, and BottleNeck were the five approaches that were used to find the top 10 genes (Supplementary table 2). CXCL8, STAT3, and STAT1 were identified as hub genes by intersecting the top 10 genes (Figure 5C-5D).

### Functional and pathway enrichment analysis of the hub genes

To investigate potential biological processes associated with ferroptosis and the development of plaque psoriasis, the hub genes were subjected to KEGG pathway enrichment and gene ontology analysis. According to GO analysis, the hub genes are primarily related to "regulation of angiogenesis, regulation of vasculature development, cytokine-mediated signaling pathway" at biological process (BP), and "chemokine receptor binding, cytokine receptor binding, G protein coupled receptor binding" at molecular function (MF). According to KEGG, the hub genes are mostly involved in the "AGE-RAGE signaling pathway in diabetic complications, Hepatitis B, Kaposi sarcoma-associated herpesvirus infection, Chemokine signaling pathway, and Coronavirus disease-COVID-19" (Figure 5E-5F). In addition, we created a KEGG heatmap of the hub genes to examine the interaction relationship (supplementary Figure 3).

### Receiver operator characteristic (ROC) curve and expression of hub genes

A ROC curve was created to verify the potential diagnostic value of the hub genes via the "pROC" package in R software 4.1.3. The AUC showed that CXCL8, STAT3 and STAT1 revealed excellent diagnostic performance for plaque psoriasis and normal tissues. The area under the ROC curve (AUC) of CXCL8, STAT3 and STAT1 was 1.0, 0.953 and 0.964 in GSE6710, and the AUC of CXCL8,

STAT3 and STAT1 was 0.764, 0.944 and 0.986 in GSE83582 (Figure 6A-6B). In GSE6710, a T-test was applied to detect the difference in hub gene expression between nonlesional and lesional skin tissue, and the results revealed that the expression of CXCL8, STAT1, and STAT3 in lesional skin tissue was significantly upregulated compared to nonlesional skin tissue. Meanwhile, in GSE83582, a T-test was applied to determine the difference in hub gene expression between healthy and lesional skin tissue, and the results indicated that STAT1 and STAT3 expression in lesional tissue was significantly upregulated compared to healthy tissue, while CXCL8 expression in lesional tissue was no different compared to healthy tissue (Figure 6C).

### Validation of the hub genes

We sought to validate our data with external datasets. To confirm that CXCL8, STAT1, and STAT3 could effectively differentiate psoriasis from controls, the diagnostic value was further validated in the GSE30999, GSE13355, and GSE78097 datasets. In the three external datasets, the three hub genes had AUC values greater than 0.75 and a maximum AUC value of 1. Further validation of the expression levels of the three hub genes was undertaken with GSE30999, GSE13355, and GSE78097, compared to control, the three hub genes expression levels in lesional skin tissue were significantly upregulated (Figure 7).

## Discussion

As far as we know, this is the first research to apply GSVA and WGCNA to construct a ferroptosis-related gene network in psoriasis. We created two ferroptosis-related gene co-expression networks in psoriasis using the WGCNA approach, and took the intersection of two key modules. Finally, we discovered three hub genes (CXCL8, STAT1, and STAT3) involved in psoriasis pathogenesis. Besides, the AUC values of three hub genes were above 0.75, which revealed a high diagnostic value. The findings of this study shed light on the molecular mechanisms behind the development of psoriasis.

Ferroptosis shares similar characteristics with psoriasis, such as increased iron buildup and enhanced lipid peroxides. The pathogenic process of ferroptosis has been reported to be directly triggered by iron excess[24]. Lipid peroxidation metabolites were found to be strongly linked to the course of psoriasis in clinical studies[25]. Furthermore, reactive oxygen species and glutathione have been discovered in the pathogenic process of psoriasis[26, 27]. However, how does ferroptosis mediate psoriasis? In psoriasis, signaling pathways associated with ferroptosis were discovered, including the lipid metabolism pathway[4]. The discovery of the mechanism of ferroptosis in psoriasis could lead to a new therapeutic target[4]. Three hub genes were discovered in this study that may be involved in the pathologic processes related to ferroptosis in psoriasis. Figure 8 depicts the potential pathways of these two genes involved in ferroptosis[28, 29], but CXCL8 remains unclear that may be associated with the Th22/Th17 pathway[4].

This research had some limitations. Firstly, while selecting datasets for Gene Set Enrichment Analysis of ferroptosis associated pathways, it was found that some datasets had few or no differences

(False Discovery Rate >0.25 or adjusted P-value >0.05), such as GSE109248, GSE79704. Therefore, we still had a limited number of datasets associated with psoriasis from which to choose. In addition, if the intersection of two ferroptosis- associated module genes was too small, the number of genes available was limited, so they couldn't be used for future research. Second, more laboratory evidence verification and literature support are needed for the possible ferroptosis-related biomarkers found in this work. Finally, the ferroptosis- associated genes are obtained from the FerrDb database, which is updated on a regular basis, and more genes are still being discovered.

To summarize, we discovered three hub genes (CXCL8, STAT1, and STAT3) that are linked to ferroptosis in psoriasis and can distinguish psoriasis from controls. As a result, CXCL8, STAT1, and STAT3 might be used as ferroptosis-associated biomarkers for disease diagnosis and treatment monitoring. However, more research into the specific molecular pathways of CXCL8, STAT1, and STAT3 for psoriasis initiation and progression is still needed.

## Appendix

Text for this section...

**Acknowledgements**
We appreciate the GEO datasets (GSE6710, GSE83582, GSE30999, GSE13355 and GSE78097) and FerrDb for free using.

**Funding**
This work was supported by the Science and Technology Project of Zengcheng District, Guangzhou (No. ZCKJ2019-005), General project of Guangdong Medical Science and Technology Research Fund (No. A2020433).

**Abbreviations**
GEO: Gene Expression Omnibus ; DEG: Differentially expressed genes ; WGCNA: Weighted gene co-expression network analysis ; GO: Gene Ontology ; KEGG: Kyoto Encyclopedia of Genes and Genomes ; ME : Module Eigengene ; BP: Biological Process ; MF: Molecular Function ; PPI: Protein-protein interaction ; ROC:Receiver Operator Characteristic; AUC: Area under curve ; GSEA: Gene Set Enrichment Analysis; GSVA: Gene Set Variation Analysis; ES: Enrichment Scores;TOM:Topological Overlap Matrixes;FDR:False Discovery Rates.

**Availability of data and materials**
The data that support the findings of this study are available in (GEO) at (https://www.ncbi.nlm.nih.gov/geo/),and a total of 259 FRGs were extracted from the FerrDb website(http://www.zhounan.org/ferrdb).

**Ethics approval and consent to participate**
Not applicable.

**Competing interests**
The authors declare that they have no competing interests.

**Consent for publication**
Not applicable.

**Authors' contributions**
All authors participated to data analysis, produced and critically evaluated the manuscript, approved the final version for publication, and agreed to be accountable for all parts of the work.

**Author details**
[1]Department of dermatology, The Fourth Affiliated Hospital of Guangzhou Medical Universitye, 511300 Guangzhou, China. [2]Department of dermatology, Zengcheng District Pepole's Hospital of Guangzhou, 511300 Guangzhou, China. [3]Department of dermatology, The fifth Affiliated Hospital of Guangzhou Medical University, 510799 Guangzhou, China.

**References**


1. Liang, H., Yan, Y., Wu, J., Ge, X., Wei, L., Liu, L., Chen, Y.: Topical nanoparticles interfering with the dna-ll37 complex to alleviate psoriatic inflammation in mice and monkeys. Science advances **6**(31), 5274 (2020)
2. Wolf, R., Mascia, F., Dharamsi, A., Howard, O.Z., Cataisson, C., Bliskovski, V., Winston, J., Feigenbaum, L., Lichti, U., Ruzicka, T., *et al.*: Gene from a psoriasis susceptibility locus primes the skin for inflammation. Science translational medicine **2**(61), 61–906190 (2010)
3. Becatti, M., Barygina, V., Mannucci, A., Emmi, G., Prisco, D., Lotti, T., Fiorillo, C., Taddei, N.: Sirt1 protects against oxidative stress-induced apoptosis in fibroblasts from psoriatic patients: A new insight into the pathogenetic mechanisms of psoriasis. International journal of molecular sciences **19**(6), 1572 (2018)
4. Shou, Y., Yang, L., Yang, Y., Xu, J.: Inhibition of keratinocyte ferroptosis suppresses psoriatic inflammation. Cell death & disease **12**(11), 1–10 (2021)
5. Lei, G., Zhang, Y., Koppula, P., Liu, X., Zhang, J., Lin, S.H., Ajani, J.A., Xiao, Q., Liao, Z., Wang, H., *et al.*: The role of ferroptosis in ionizing radiation-induced cell death and tumor suppression. Cell research **30**(2), 146–162 (2020)
6. Cheng, Y., Qu, W., Li, J., Jia, B., Song, Y., Wang, L., Rui, T., Li, Q., Luo, C.: Ferristatin ii, an iron uptake inhibitor, exerts neuroprotection against traumatic brain injury via suppressing ferroptosis. ACS Chemical Neuroscience **13**(5), 664–675 (2022)
7. Shen, L., Lin, D., Li, X., Wu, H., Lenahan, C., Pan, Y., Xu, W., Chen, Y., Shao, A., Zhang, J.: Ferroptosis in acute central nervous system injuries: the future direction? Frontiers in cell and developmental biology **8**, 594 (2020)
8. Chen, X., Li, X., Xu, X., Li, L., Liang, N., Zhang, L., Lv, J., Wu, Y.-C., Yin, H.: Ferroptosis and cardiovascular disease: role of free radical-induced lipid peroxidation. Free Radical Research **55**(4), 405–415 (2021)
9. Linkermann, A., Skouta, R., Himmerkus, N., Mulay, S.R., Dewitz, C., De Zen, F., Prokai, A., Zuchtriegel, G., Krombach, F., Welz, P.-S., *et al.*: Synchronized renal tubular cell death involves ferroptosis. Proceedings of the National Academy of Sciences **111**(47), 16836–16841 (2014)
10. Bai, Q., Liu, J., Wang, G.: Ferroptosis, a regulated neuronal cell death type after intracerebral hemorrhage. Frontiers In Cellular Neuroscience, 374 (2020)
11. Hurgobin, B., de Jong, E., Bosco, A.: Insights into respiratory disease through bioinformatics. Respirology **23**(12), 1117–1126 (2018)
12. Hong, M., Tao, S., Zhang, L., Diao, L.-T., Huang, X., Huang, S., Xie, S.-J., Xiao, Z.-D., Zhang, H.: Rna sequencing: new technologies and applications in cancer research. Journal of hematology & oncology **13**(1), 1–16 (2020)
13. Langfelder, P., Horvath, S.: Wgcna: an r package for weighted correlation network analysis. BMC bioinformatics **9**(1), 1–13 (2008)
14. Gautier, L., Cope, L., Bolstad, B.M., Irizarry, R.A.: affy—analysis of affymetrix genechip data at the probe level. Bioinformatics **20**(3), 307–315 (2004)
15. Zhou, N., Bao, J.: Ferrdb: a manually curated resource for regulators and markers of ferroptosis and ferroptosis-disease associations. Database **2020** (2020)
16. Ritchie, M.E., Phipson, B., Wu, D., Hu, Y., Law, C.W., Shi, W., Smyth, G.K.: limma powers differential expression analyses for rna-sequencing and microarray studies. Nucleic acids research **43**(7), 47–47 (2015)
17. Yu, G., Wang, L.-G., Han, Y., He, Q.-Y.: clusterprofiler: an r package for comparing biological themes among gene clusters. Omics: a journal of integrative biology **16**(5), 284–287 (2012)
18. Subramanian, A., Tamayo, P., Mootha, V.K., Mukherjee, S., Ebert, B.L., Gillette, M.A., Paulovich, A., Pomeroy, S.L., Golub, T.R., Lander, E.S., *et al.*: Gene set enrichment analysis: a knowledge-based approach for interpreting genome-wide expression profiles. Proceedings of the National Academy of Sciences **102**(43), 15545–15550 (2005)
19. Hänzelmann, S., Castelo, R., Guinney, J.: Gsva: gene set variation analysis for microarray and rna-seq data. BMC bioinformatics **14**(1), 1–15 (2013)
20. Szklarczyk, D., Franceschini, A., Wyder, S., Forslund, K., Heller, D., Huerta-Cepas, J., Simonovic, M., Roth, A., Santos, A., Tsafou, K.P., *et al.*: String v10: protein–protein interaction networks, integrated over the tree of life. Nucleic acids research **43**(D1), 447–452 (2015)
21. Shannon, P., Markiel, A., Ozier, O., Baliga, N.S., Wang, J.T., Ramage, D., Amin, N., Schwikowski, B., Ideker, T.: Cytoscape: a software environment for integrated models of biomolecular interaction networks. Genome research **13**(11), 2498–2504 (2003)
22. Chin, C.-H., Chen, S.-H., Wu, H.-H., Ho, C.-W., Ko, M.-T., Lin, C.-Y.: cytohubba: identifying hub objects and sub-networks from complex interactome. BMC systems biology **8**(4), 1–7 (2014)
23. Nahm, F.S.: Receiver operating characteristic curve: overview and practical use for clinicians. Korean journal of anesthesiology **75**(1), 25–36 (2022)
24. Huang, S., Cao, B., Zhang, J., Feng, Y., Wang, L., Chen, X., Su, H., Liao, S., Liu, J., Yan, J., *et al.*: Induction of ferroptosis in human nasopharyngeal cancer cells by cucurbitacin b: molecular mechanism and therapeutic potential. Cell death & disease **12**(3), 1–13 (2021)
25. Wójcik, P., Biernacki, M., Wroński, A., Łuczaj, W., Waeg, G., Žarković, N., Skrzydlewska, E.: Altered lipid metabolism in blood mononuclear cells of psoriatic patients indicates differential changes in psoriasis vulgaris and psoriatic arthritis. International journal of molecular sciences **20**(17), 4249 (2019)
26. Hoffmann, J., Schaekel, K., Hartl, D., Enk, A., Hadaschik, E.: Dimethyl fumarate modulates neutrophil extracellular trap formation in a glutathione-and superoxide-dependent manner. British Journal of Dermatology **178**(1), 207–214 (2018)
27. Kaur, S., Zilmer, K., Kairane, C., Kals, M., Zilmer, M.: Clear differences in adiponectin level and glutathione redox status

revealed in obese and normal-weight patients with psoriasis. British Journal of Dermatology **159**(6), 1364–1367 (2008)
28. Wei, T.-T., Zhang, M.-Y., Zheng, X.-H., Xie, T.-H., Wang, W., Zou, J., Li, Y., Li, H.-Y., Cai, J., Wang, X., et al.: Interferon-$\gamma$ induces retinal pigment epithelial cell ferroptosis by a jak1-2/stat1/slc7a11 signaling pathway in age-related macular degeneration. The FEBS journal (2021)
29. Zhou, B., Liu, J., Kang, R., Klionsky, D.J., Kroemer, G., Tang, D.: Ferroptosis is a type of autophagy-dependent cell death. In: Seminars in Cancer Biology, vol. 66, pp. 89–100 (2020). Elsevier

**Figures**

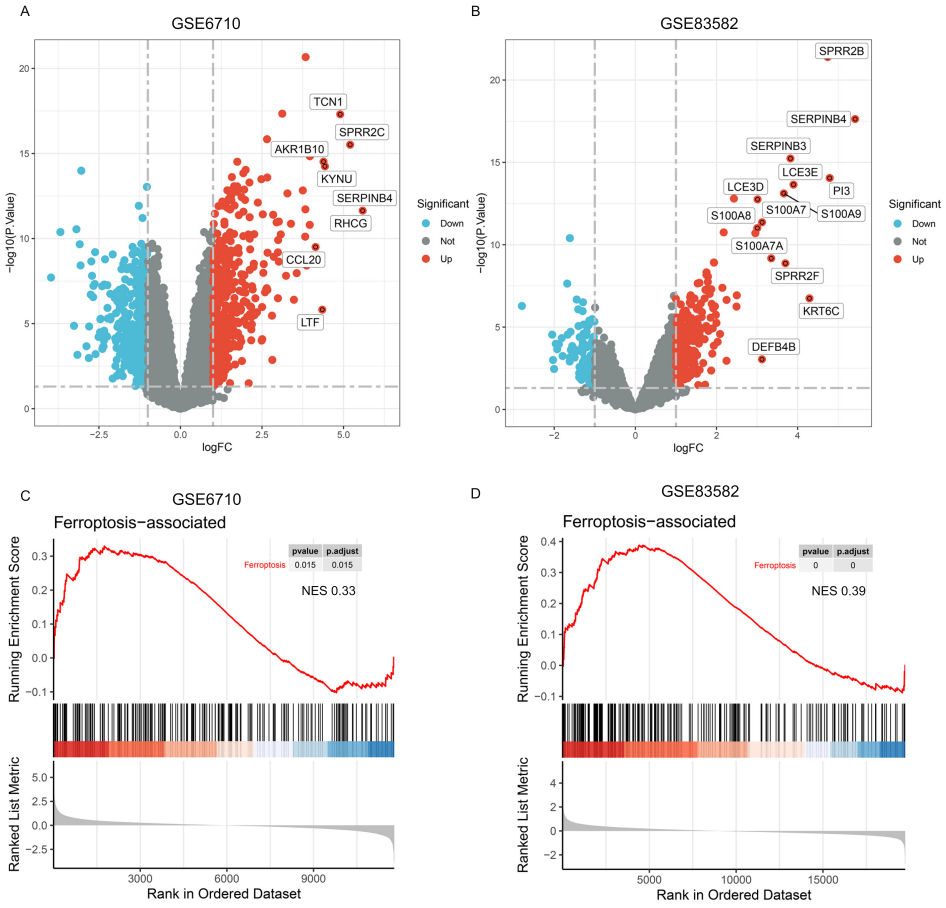


**Figure 1** In GSE6710 and GSE83582 datasets, differentially expressed genes (DEGs) and gene set enrichment analysis (GSEA) of ferroptosis-associated pathways. (A-B) Identification of DEGs in GSE6710 and GSE83582. All DEGs are plotted as volcano maps. Up-regulated genes are shown by red dots, down-regulated genes are represented by blue dots, and unaltered genes are represented by grey dots The DEGs with the most aberrantly expression were highlighted; (C-D) Gene set enrichment analysis of ferroptosis-associated pathways on the transcriptomic data in GSE6710 and GSE83582 performed, in these graphs, the red line indicates the running enrichment score, and the black bars delineates the location of gene set members in the sequenced expression data.

**Additional Files**

Additional file 1 — Additional Figure1
The flowchart of this research.

Additional file 2 — Additional Figure2
The 10 modules and the eigengene network heatmap in GSE6710.

Additional file 3 — Additional Figure3
The KEGG heatmap of the hub genes.

Additional file 4 — Additional table1
The ES of each gene set that was connected to ferroptosis pathways was obtained using GSVA.

Additional file 5 — Additional table2
Top 10 genes by five approaches.

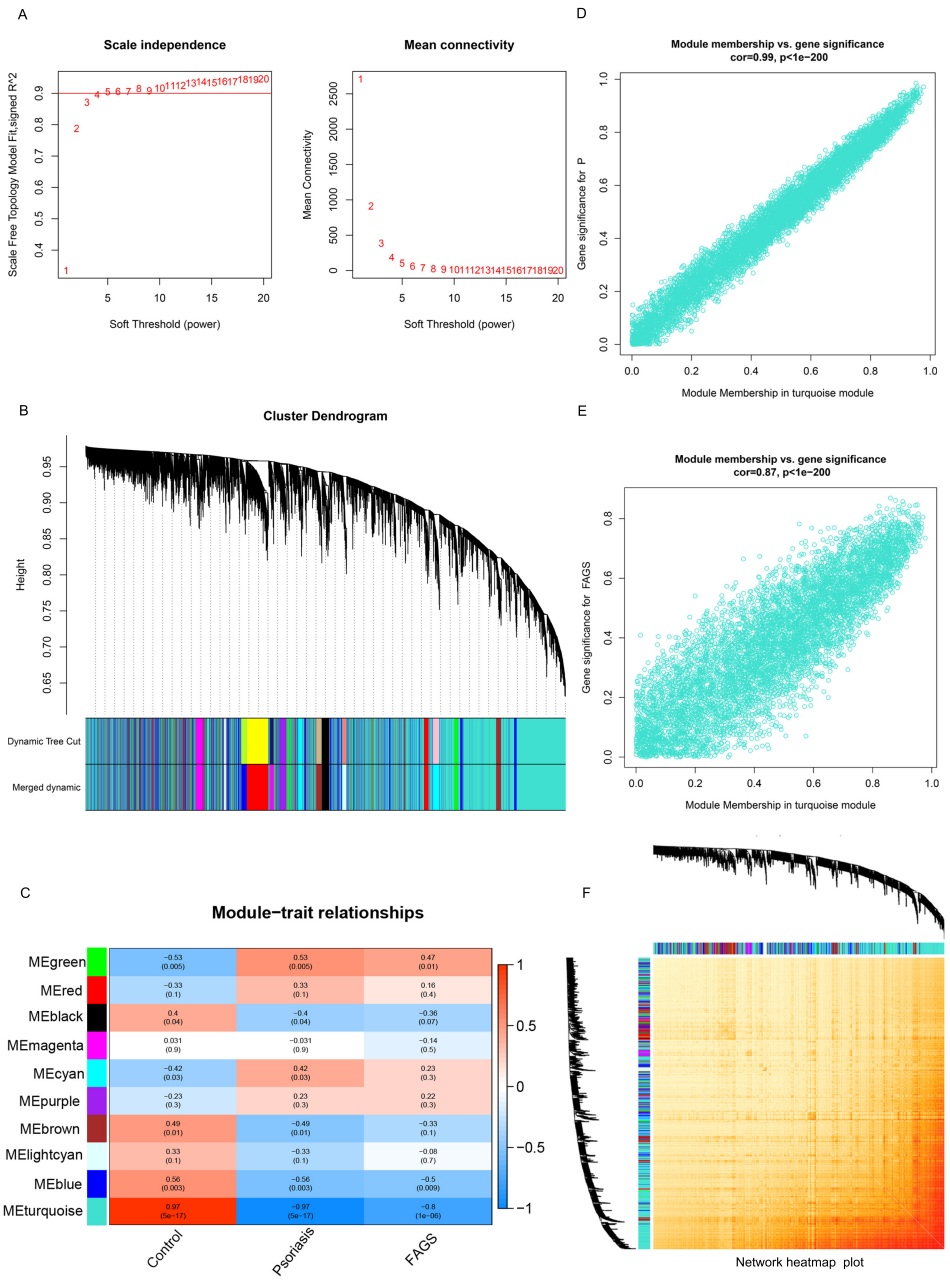


**Figure 2** Weighted gene co-expression network analysis of GSE6710. (A)The scale-free fit index on the left and the average connectivity on the right are used to analyze various soft threshold capabilities; (B)GSE6710 gene clustering dendrogram based on the dissimilarity TOM (1-TOM). Each branch represents a gene, and each color below represents a co-expression module; (C) The correlation between each module and feature. Each row represents a module eigengene, and each column represents a clinic characteristic. Each cell contains the p-value and correlation for each module; (D-E) In the turquoise module, a scatter plot showing eigengene importance vs modular membership. Intra-module analysis found in the turquoise module revealed a strong link to psoriasis and ferroptosis, respectively with and a p value of 1e-200 ang a correlation of 0.99, and a p value of 1e-200 and a correlation of 0.87; (F) To show the module structure, a heatmap of selected 1000 genes randomly was used to create a TOM plot. The light-yellow hue in the TOM plot suggests minimal overlap, whereas the deeper yellow tint indicates larger overlap. The gene dendrogram is shown on the left sides of the heatmap and the module assignment is shown on the top sides of the heatmap.

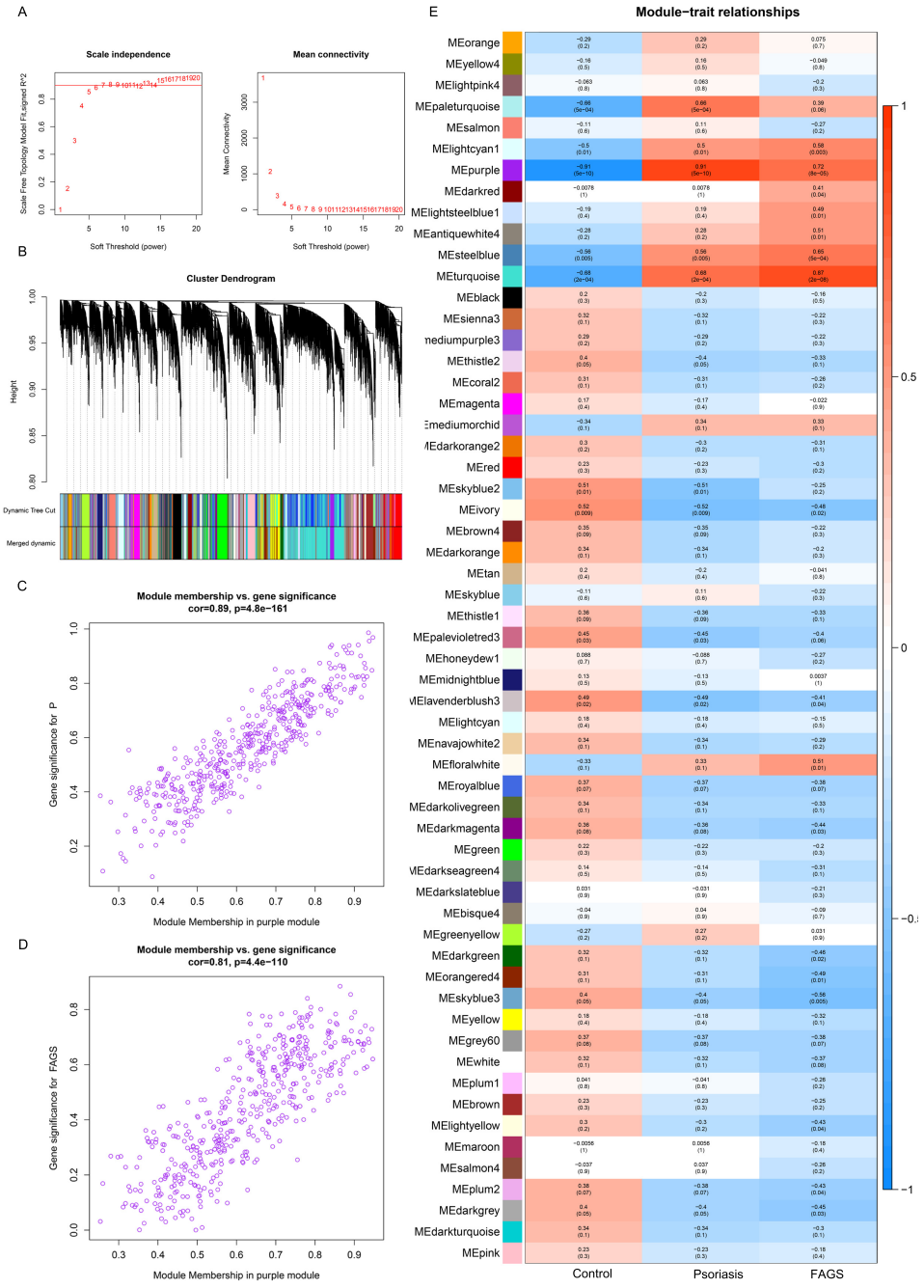


**Figure 3** Weighted gene co-expression network analysis of GSE83582. (A) The scale-free fit index on the left and the average connectivity on the right are used to analyze various soft threshold capabilities; (B)GSE83582 gene clustering dendrogram based on the dissimilarity TOM (1-TOM). Each branch represents a gene, and each color below represents a co-expression module; (C-D) In the purple module, a scatter plot showing eigengene importance vs modular membership. Intra-module analysis found in the purple module revealed a strong link to psoriasis and ferroptosis, respectively with and a p value of 4.8e-161 and a correlation of 0.89, and a p value of 4.4e-110 and a correlation of 0.81; (E) The correlation between each module and feature. Each row represents a module eigengene, and each column represents a clinic characteristic. Each cell contains the p-value and correlation for each module.

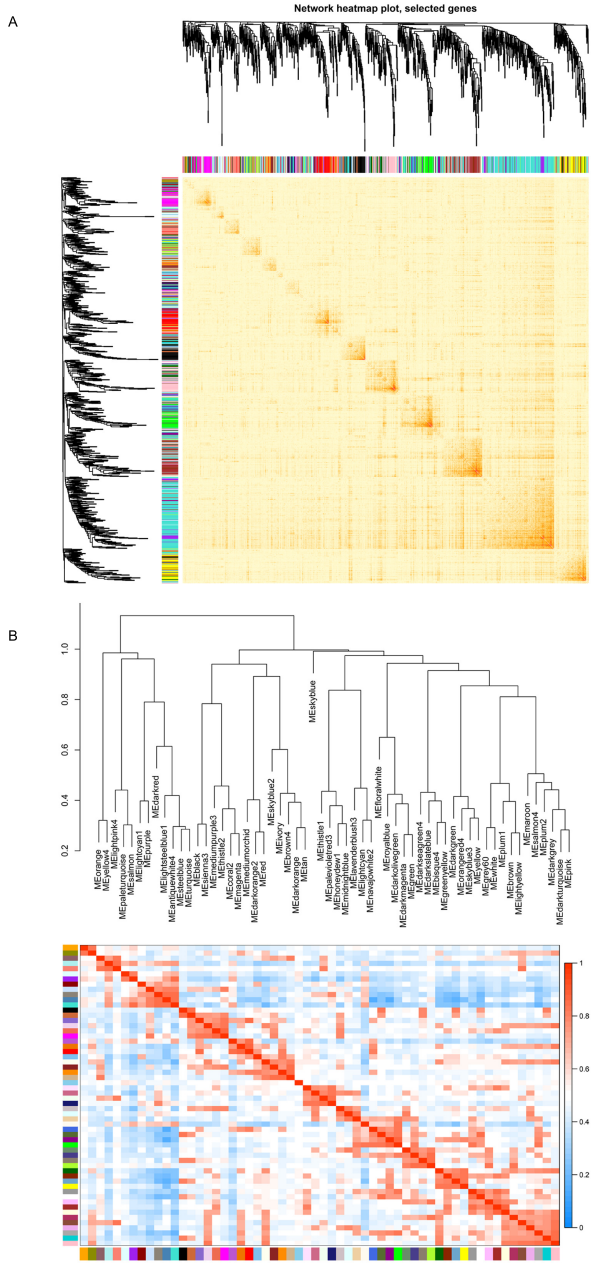


**Figure 4** Weighted gene co-expression network analysis of GSE83582. (A) To show the module structure, a heatmap of selected randomly 1000 genes was used to create a TOM plot. The light-yellow hue in the TOM plot suggests minimal overlap, whereas the deeper yellow tint indicates larger overlap. The gene dendrogram is shown on the left sides of the heatmap and the module assignment is shown on the top sides of the heatmap; (B) The eigengene network heatmap and the module eigengene dendrogram summarize the modules produced in the clustering analysis.

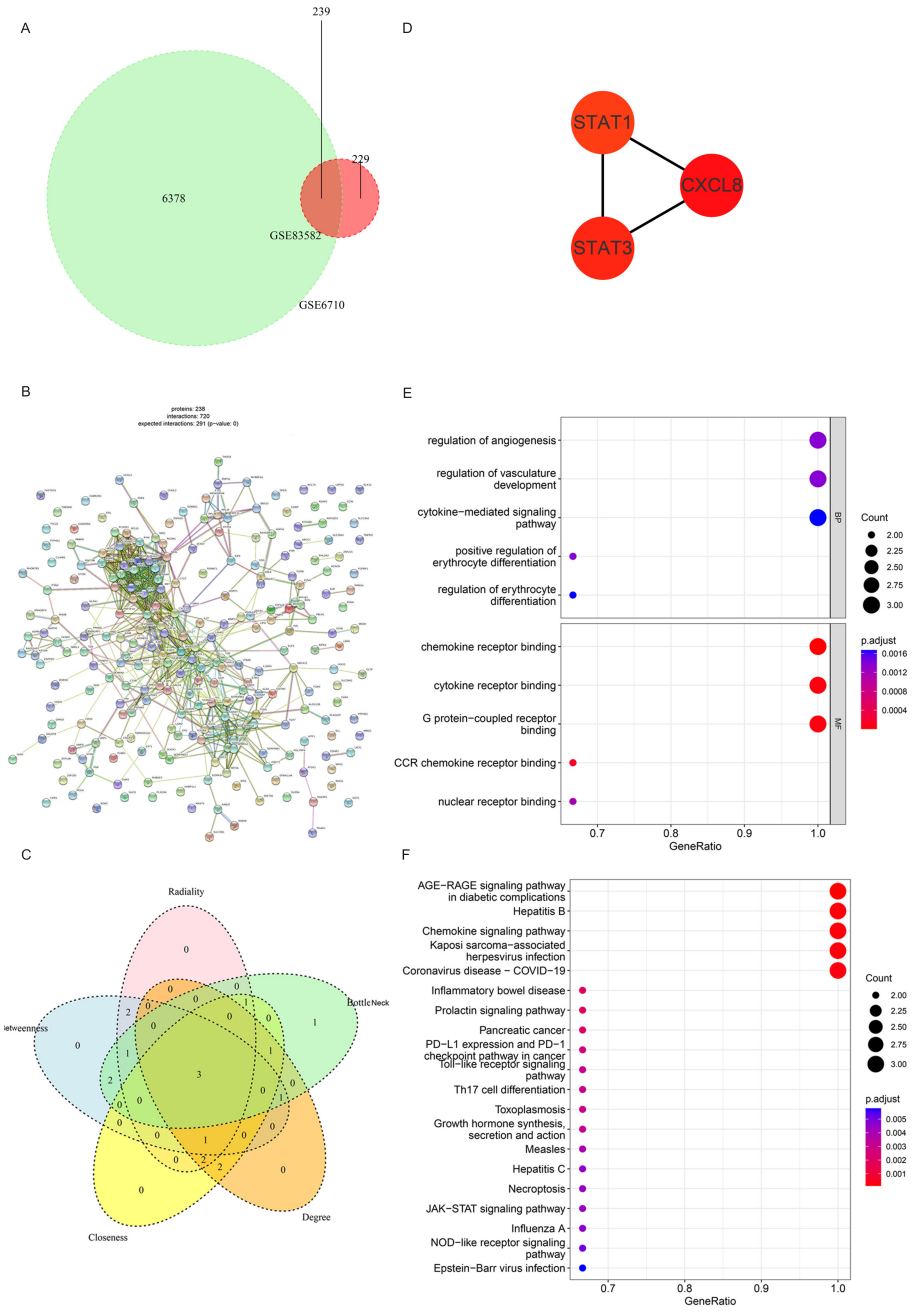


**Figure 5** Hub gene identification and functional enrichment analysis.(A)The intersection genes of the turquoise module in GSE6710 and the purple module in GSE83582 are presented in the Venn diagram; (B)STRING database evaluated the protein-protein interaction networks of 239 genes; (C)Venn diagram illustrates the intersection genes of the top 10 genes which were obtained by the Cytoscape plug-in CytoHubba, Radiality, Betweenness, Closeness, Degre, and BottleNeck were the five approaches that were applied to find the top 10 genes; (D)By intersecting the top ten genes, the three hub genes were discovered; (E-F) For the three hub genes, BP (biological process) terms, MF(molecular function) terms and KEGG analysis were applied.

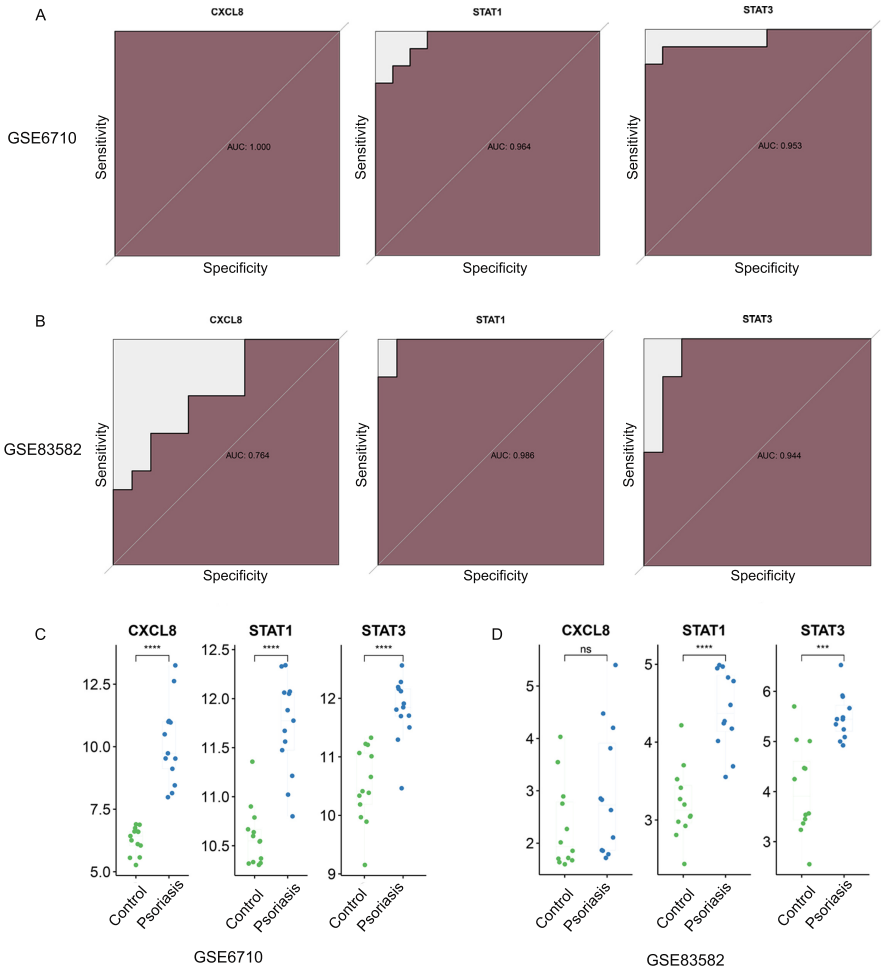


**Figure 6** ROC curve and the gene expression levels of CXCL8, STAT1, STAT3 in GSE6710 and GSE83582. (A-B) In GSE6710 and GSE83582, the ability to identify psoriasis from healthy controls with high sensitivity and specificity is assessed using ROC(receiver operating characteristic) curves and (AUC)area under the curve; (C) CXCL8, STAT1 and STAT3 are greatly upregulated in GSE6710 compared with control, and STAT1 and STAT3 are greatly upregulated in GSE83582 compared with control(ns p >0.05; *p <0.05; **p <0.01; ***p <0.001; ****p <0.0001).

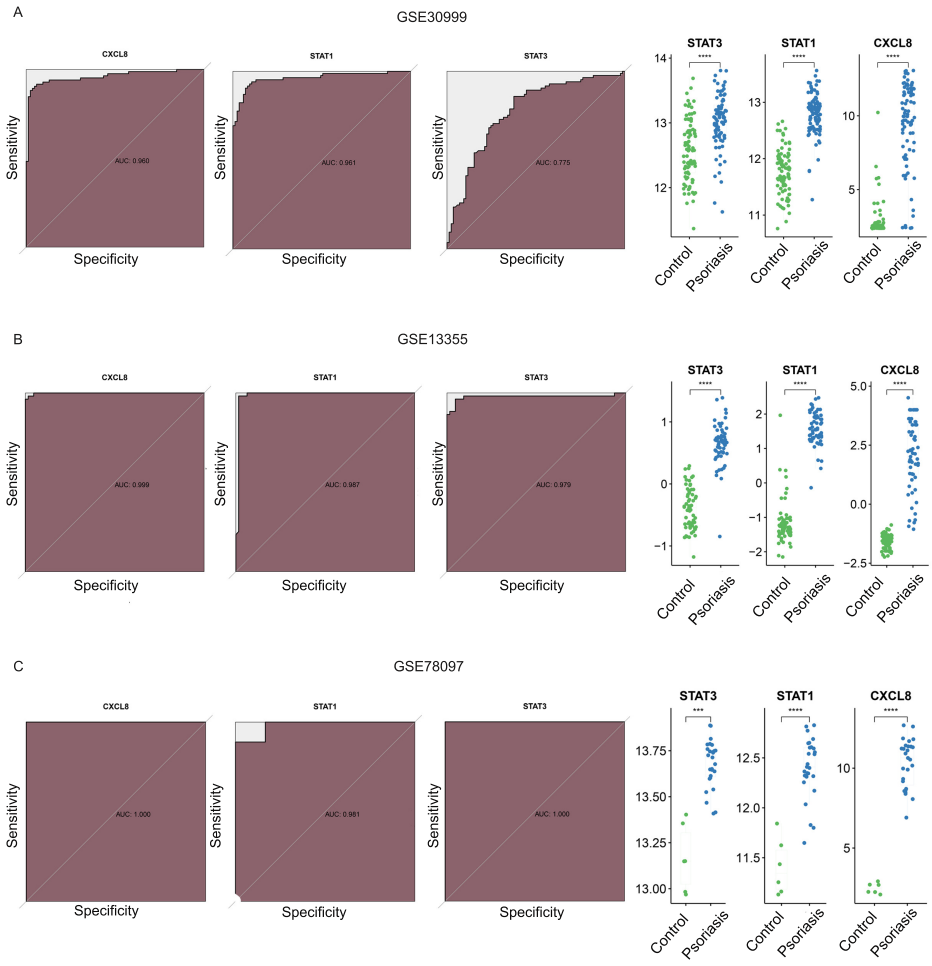


**Figure 7** Validation of the three hub genes in external datasets. (A) Validation of CXCL8, STAT1, STAT3 in the dataset of GSE30999; (B) Validation of CXCL8, STAT1, STAT3 in the dataset of GSE13355; (C) Validation of CXCL8, STAT1, STAT3 in the dataset of GSE78097.

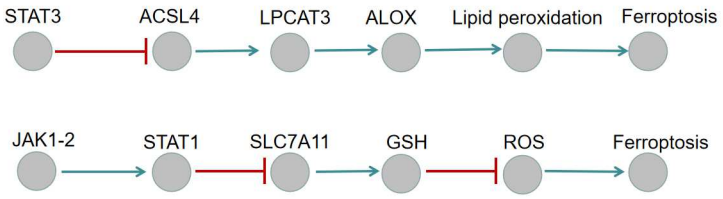


**Figure 8** The regulation pathways of STAT1 and STAT3 participating in ferroptosis in psoriasis. Suppression is represented by the red T-shaped edge, while promotion is represented by the blue arrow.

# Supplementary Files

This is a list of supplementary files associated with this preprint. Click to download.

- AdditionalTable1.xls
- AdditionalTable2.xls
- AdditionalFigure1.eps
- AdditionalFigure2.eps
- AdditionalFigure3.eps